

# 1 Role of Potassium and Calcium on the Combustion Characteristics of 2 Biomass Obtained from Thermogravimetric Experiments

3 M. Abián,<sup>\*,†</sup> M. U. Alzueta,<sup>†</sup> A. Carvalho,<sup>‡</sup> M. Rabaçal,<sup>‡</sup> and M. Costa<sup>‡</sup>

4 <sup>†</sup>Aragón Institute of Engineering Research (I3A), Department of Chemical and Environmental Engineering, University of Zaragoza,  
5 50018 Zaragoza, Spain

6 <sup>‡</sup>Institute of Mechanical Engineering (IDMEC), Mechanical Engineering Department, Instituto Superior Técnico, Universidade de  
7 Lisboa, 1049-001 Lisboa, Portugal

8  Supporting Information

9 **ABSTRACT:** This work focuses on the combustion behavior of raw and demineralized grape pomace and grape pomace doped  
10 with 0.1, 0.5, 0.82 (equal to the K concentration in the raw biomass), 3, and 6 wt % K and 0.1, 0.5, 1.08 (equal to the Ca  
11 concentration in the raw biomass), 3, and 6 wt % Ca. To identify the individual role of calcium and potassium, the biomass  
12 samples were either pyrolyzed in a N<sub>2</sub> atmosphere or oxidized in air in a thermogravimetric analyzer (TGA) during non-  
13 isothermal runs at 10 K/min from room temperature to a maximum temperature of 1275 K. In all of the cases, the biomass  
14 pyrolysis process shows one main stage associated with the volatile matter release. This process is not significantly affected by the  
15 mineral content of biomass nor the presence of high K and Ca contents. During combustion in air, the biomass samples show  
16 two main distinct stages that are associated with the volatile matter release and the char oxidation. Whereas the main  
17 devolatilization stage is not significantly affected by the mineral content of the biomass, the char oxidation stage is shifted to  
18 higher temperatures for the demineralized biomass. Potassium and calcium play a different role on the char oxidation process. In  
19 general, char oxidation is promoted with increasing the K content, whereas Ca does not significantly influences this process. The  
20 TGA results were also used to determine the kinetic parameters of the pyrolysis and combustion processes of biomass in the  
21 presence of K and Ca.

## 1. INTRODUCTION

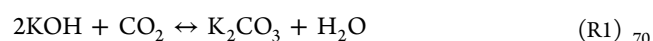
22 The use of biomass in combustion has increased over the last  
23 few decades because it is considered as a renewable and CO<sub>2</sub>-  
24 neutral energy source. However, despite the growing develop-  
25 ment of different technologies for the thermochemical  
26 conversion of biomass, there are still issues, such as preparation  
27 of biomass and/or ash-related matters during and after  
28 combustion, that hinder the clean and efficient utilization of  
29 biomass in energy applications.<sup>1</sup> In particular, the presence of  
30 metals, even in small quantities, may affect the overall  
31 combustion process and the formation of pollutants.<sup>2</sup>

32 The pyrolysis of solid fuels produces volatiles and char,  
33 which, in turn, result from both the direct primary  
34 decomposition of the solid fuel and the secondary reactions  
35 of volatile condensable organic products.<sup>3</sup> During combustion,  
36 the decomposition of the organic structures of biomass is  
37 accompanied by the release of its mineral constituents. Once  
38 released, the metals can be transported in the combustion gas  
39 as either solid particles or vapor species,<sup>1</sup> depending upon the  
40 given element considered. Although the mineral content  
41 depends upon the type of biomass (e.g., refs 4 and 5),  
42 potassium (K) is typically the main alkali earth metal and  
43 calcium (Ca) is the main alkaline metal present in biomass.<sup>6</sup>  
44 Usually, K is regarded as an undesirable biomass component as  
45 a result of its critical role in important ash-related problems  
46 (e.g., alkali-induced slagging, silicate melt-induced slagging, ash  
47 fusion, and bed agglomeration).<sup>1,7</sup> In contrast and despite the  
48 calcium sulfate deposits found on the cold reactor surfaces, Ca  
49 can inhibit the occurrence of silicate melt-induced slagging and

bed agglomeration as a result of the formation of melting  
calcium potassium phosphates and silicates at high temper-  
atures.<sup>1,8,9</sup>

K is mostly present in biomass in a soluble form (e.g., in an  
ionic form in salts or as organically bound K ions).<sup>1</sup> Two  
characteristic temperature intervals have been identified for the  
release of K, as alkali metal, during biomass pyrolysis.<sup>10</sup> K  
associated with the organic phase is expected to be released  
coinciding with the onset of the pyrolysis process (453–773  
K), whereas inorganic K, from the ash component of the  
resulting char, would be released at higher temperatures (>773  
K).

During combustion, soluble K is mainly released to the gas  
phase as K(g), KOH(g), and KCl(g) provided that Cl is  
available. Subsequently, these K species can interact with other  
compounds through different reactions depending upon the  
given reaction environment. In the absence of chlorine and  
sulfur, possible reactions include the interaction of K(g) with  
water vapor to form KOH(g) and the subsequent carbonation  
of hydroxide at temperatures below 1073 K.<sup>11</sup>



At high enough temperatures (i.e., 1180 K), potassium  
carbonate can decompose through reaction R2.<sup>12</sup>

Received: July 24, 2017

Revised: September 27, 2017

Published: September 28, 2017



74 The presence of K during biomass conversion in the form of  
75 either KOH,<sup>13</sup> K<sub>2</sub>CO<sub>3</sub>,<sup>14</sup> potassium acetate,<sup>15</sup> or potassium  
76 carboxylates<sup>16</sup> promotes the char formation.

77 In addition, K can also act as a catalyst for the devolatilization  
78 and char combustion stages of biomass.<sup>10,17–20</sup>

79 Ca can be found in biomass in three forms: organically  
80 bound, acid soluble, and acid insoluble. Under combustion  
81 conditions, acid-insoluble Ca (e.g., Ca silicates) is usually  
82 considered inert, whereas organically bound and acid-soluble  
83 Ca are readily converted into CaO.<sup>1</sup> Within the combustion  
84 chamber, CaO exists as refractory small micrometer-sized  
85 particles and will stay as is provided that it is not participating  
86 in further reactions.<sup>21</sup> In general, literature works point to a  
87 negligible influence of Ca on the main pyrolysis products of  
88 biomass.<sup>22,23</sup> However, the addition of Ca as either CaCO<sub>3</sub><sup>24,25</sup>  
89 or CaO<sup>25,26</sup> can increase the char combustion rate.

90 Even though K and Ca can catalyze the biomass conversion  
91 during both pyrolysis and combustion processes,<sup>18</sup> the relative  
92 magnitude of the effect depends upon the given metal. In this  
93 way, previous studies highlight the higher catalytic activity of K  
94 compared to Ca.<sup>27</sup>

95 In this context, the aim of this work is to investigate the  
96 impact of the presence and concentration of K and Ca on the  
97 devolatilization and char oxidation characteristics of biomass  
98 fuels, taking as a reference point grape pomace biomass. The  
99 reference biomass was demineralized and subsequently doped  
100 with different concentrations of K (using potassium oxalate  
101 monohydrate as a reactant) and Ca (using calcium oxalate  
102 monohydrate as a reactant), making a total of 12 different  
103 samples. Both pyrolysis and combustion behaviors have been  
104 examined in a thermogravimetric analyzer (TGA), and the  
105 effects of the presence of the minerals on the sample reactivity  
106 was analyzed. To this end, the characteristic temperatures of the  
107 initial stage, the peak rate, and the final stage were compared  
108 for the different biomass samples for both conversion processes.  
109 Additionally, the minimum ignition temperature was estimated  
110 using three different graphical methods. Finally, the activation  
111 energies of the pyrolysis process and the devolatilization and  
112 char oxidation stages in the case of combustion were estimated  
113 using an optimization procedure.

## 2. MATERIALS AND METHODS

114 **2.1. Sample Preparation.** In this study, grape pomace biomass  
115 has been selected as the reference biomass. Grape pomace is a residue  
116 generated during the wine production, and it is mainly constituted by  
117 skins and seeds. Table 1 lists the main properties of the grape pomace  
118 biomass, and Figure 1 provides its particle size distribution.

119 To prepare the different samples, the raw grape pomace was first  
120 demineralized by a nitric-acid-leaching procedure.<sup>28</sup> In particular, 30 g  
121 of raw biomass was placed in a flask with 500 mL of ion-exchanged  
122 water. pH of the dissolution was adjusted to 2 using HNO<sub>3</sub> and stirred  
123 for 1 h at 60 °C. Subsequently, the biomass was filtered and washed  
124 thoroughly with 200 mL of ion-exchanged water. The filtering–  
125 washing procedure was repeated 4 times. Finally, the biomass was  
126 dried at 105 °C. The complete procedure was repeated twice.

127 Afterward, the demineralized biomass was impregnated with  
128 different concentrations of either K (using potassium oxalate  
129 monohydrate as a reactant) or Ca (using calcium oxalate monohydrate  
130 as a reactant). The wet impregnation procedure consists of adding  
131 different amounts of K or Ca reactant to ion-exchange water to obtain  
132 the desired concentrations of K or Ca in the dissolutions.  
133 Subsequently, 11 mL of each dissolution was mixed with 5 g of

**Table 1. Properties of the Raw Grape Pomace Biomass**

parameter	value
Proximate Analysis (wt %, As Received)	
volatiles	48.4
fixed carbon	18.6
moisture	30.2
ash	2.8
Ultimate Analysis (wt %, Dry and Ash-Free Basis)	
carbon	51.1
hydrogen	6.7
nitrogen	1.9
sulfur	0.2
oxygen	40.1
Heating Value (MJ/kg)	
high	21.2
low	19.8
Ash Analysis (wt %, Dry Basis)	
SiO <sub>2</sub>	5.5
Al <sub>2</sub> O <sub>3</sub>	1.0
Fe <sub>2</sub> O <sub>3</sub>	1.2
CaO	37.8
SO <sub>3</sub>	1.7
MgO	7.2
P <sub>2</sub> O <sub>5</sub>	19.7
K <sub>2</sub> O	24.7
Na <sub>2</sub> O	0.4
other oxides	0.8

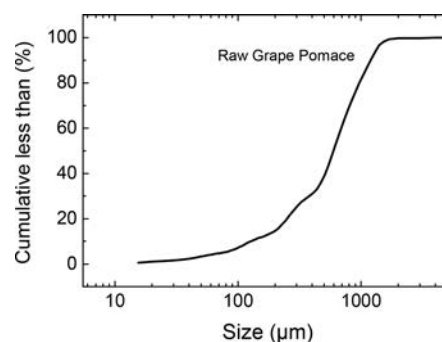


**Figure 1.** Particle size distribution of the raw grape pomace.

demineralized biomass. The resultant impregnated biomass samples  
134 were dried at 105 °C and stored at ambient conditions. 135

The specific K and Ca reactant amounts were selected to cover a  
136 wide and realistic range of K and Ca concentrations in different  
137 biomass residues (see the work of Tortosa-Masiá et al.<sup>4</sup>). Thus, the  
138 present work includes the analysis of the pyrolysis and oxidation  
139 behaviors of raw and demineralized grape pomace and grape pomace  
140 doped with 0.1, 0.5, 0.82 (equal to the K concentration in the raw  
141 biomass), 3, and 6 wt % K and 0.1, 0.5, 1.08 (equal to the Ca  
142 concentration in the raw biomass), 3, and 6 wt % Ca. 143

**2.2. Thermogravimetric Tests.** The evaluation of the combustion  
144 behavior of biomass is based on the measurement of the mass change  
145 in a sample as a function of the temperature and time at a constant  
146 heating rate of 10 K/min from room temperature up to 1275 K in  
147 either nitrogen or air, using a NETZSCH STA F1 Jupiter TGA. The  
148 experiments were performed at atmospheric pressure using alumina  
149 crucibles and 5 mg of each biomass sample. The initial sample mass  
150 and heating rate used in these tests were chosen based on previous  
151 studies addressing the pyrolysis and combustion behaviors of different  
152 biomass residues in TGA experiments.<sup>29,30</sup> Prior to the experiments,  
153 for each experimental condition (i.e., air or N<sub>2</sub> atmosphere), a 154

155 calibration curve was made to avoid possible fluctuations caused by the  
156 apparatus that could influence the measurements.

157 The figures show the biomass pyrolysis and combustion reactivities  
158 as the mass loss rate,  $dX/dt$  ( $\text{min}^{-1}$ ), defined through eq 1, versus the  
159 reaction temperature,  $T$  (K).

$$160 \quad \frac{dX}{dt} = \frac{1}{m_0} \frac{dm}{dt} \quad (1)$$

161 Here,  $m_0$  and  $m$  are the initial mass of biomass and the mass of  
162 biomass at time  $t$  in the TGA tests, respectively. Thus, the biomass  
163 conversion,  $X$ , is defined by

$$164 \quad X = \frac{m_0 - m}{m_0} \quad (2)$$

165 To determine the uncertainty in the experimental procedure, the  
166 experiments were repeated at least 3 times. In addition, to disregard  
167 the possible influence of the biomass size distribution on the TGA  
168 results, the samples were sieved into the 200–250  $\mu\text{m}$  size interval  
169 and, subsequently, subjected to the pyrolysis and combustion tests. As  
170 an example of the comparison results obtained, Figure 2 shows the

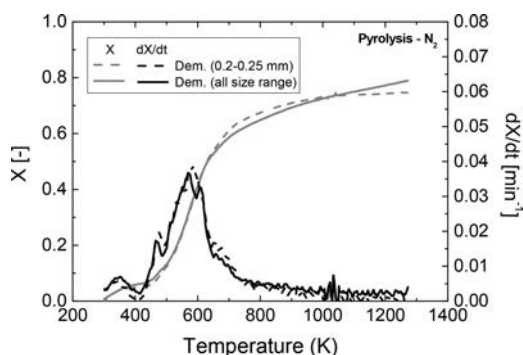


Figure 2. Typical pyrolysis profiles of the demineralized grape pomace.

171 conversion  $X$  and the rate of mass loss  $dX/dt$  for the pyrolysis of the  
172 demineralized biomass. The similitude of results is high, indicating a  
173 good repeatability of the procedure and a low effect of the biomass size  
174 distribution of the samples under the conditions of the present work.

175 **2.3. Pyrolysis and Combustion Modeling.** The TGA results  
176 were used to determine the kinetic parameters of the pyrolysis and  
177 combustion processes of biomass in the presence of K and Ca. This  
178 analysis was carried out using the fitting procedure developed by  
179 Ferreiro et al.<sup>30</sup> The method includes a combined genetic algorithm  
180 from the global optimization toolbox of MATLAB and the least  
181 squares (LSQ) fitting procedure of MATLAB for the estimation of the  
182 activation energy and pre-exponential factor of both pyrolysis and  
183 combustion of biomass through the use of a single first-order reaction  
184 model. A detailed description of the procedure can be found  
185 elsewhere.<sup>30</sup>

186 Both pyrolysis and devolatilization are modeled using a single first-  
187 order reaction.<sup>3</sup> The reaction rate is defined as a function of the  
188 temperature and degree of conversion through eq 3

$$189 \quad \frac{dm}{dt} = k(T_p)(VM - V_g) \quad (3)$$

190 where  $dm/dt$  is the mass in weight percent at time  $t$ ,  $T_p$  is the particle  
191 temperature,  $VM$  is the maximum volatile matter in weight percent  
192 that can be lost,  $V_g$  is the total amount of volatile gases in weight  
193 percent that have left the particle, and  $k(T)$  is the rate constant  
194 expressed by the Arrhenius equation (eq 4)

$$195 \quad k_V = A_V T_p^\gamma \exp\left(\frac{-E_V}{RT_p}\right) \quad (4)$$

where  $R$  is the ideal gas constant ( $\text{J K}^{-1} \text{mol}^{-1}$ ),  $A_V$  is the pre-  
exponential factor ( $\text{s}^{-1}$ ),  $E_V$  is the activation energy ( $\text{J/mol}$ ), and  $\gamma$  is  
the temperature power coefficient.

Char combustion is modeled using a single reaction as well.<sup>31</sup> The  
reaction rate is defined as a function of the temperature, concentration  
of the oxidizer, and degree of conversion through eq 5

$$202 \quad \frac{dX}{dt} = k(T_p) P_{\text{O}_2}^n (1 - X) \quad (5)$$

where  $X$  is the biomass conversion,  $P_{\text{O}_2}$  is the partial pressure of the  
oxidizer, and  $n$  is the reaction order. The rate constant is also  
expressed by a variation of the Arrhenius equation

$$206 \quad k_C = A_C \exp\left(\frac{-E_C}{RT_p}\right) \quad (6)$$

In the case of combustion, the total mass loss is defined as the  
summation of the devolatilization and the char combustion rate.

The kinetic parameters considered for fitting are  $A_V$ ,  $\gamma$ ,  $E_C$ ,  $A_C$ ,  $E_V$ ,  
and  $n$ . The reaction order  $n$  was limited to the typical values for the  
temperatures used in thermogravimetric analysis (i.e., from 0.5 to 1),  
and the temperature power coefficients were limited to the  $-10$  to  $10$   
universe values.<sup>30</sup> The evaluation function to be minimized by the  
genetic algorithm followed a similar form as that used in the work of  
Ferreiro et al.<sup>30</sup> Here, the global error is defined as a combination of  
(i) the error between the predicted and experimental mass loss curve  
(TG) and (ii) the characteristic temperature of the maximum peaks of  
the rate curve (DTG). In the case of combustion, two peaks are  
considered: the maximum devolatilization peak and the maximum char  
combustion peak.

As an example of the qualitative interpretation of the biomass  
pyrolysis and combustion profiles, Figure 3 shows the experimental and  
model prediction results for the demineralized biomass. The  
pyrolysis and combustion models capture, in general, well the overall  
behavior of the biomass devolatilization and char oxidation processes.

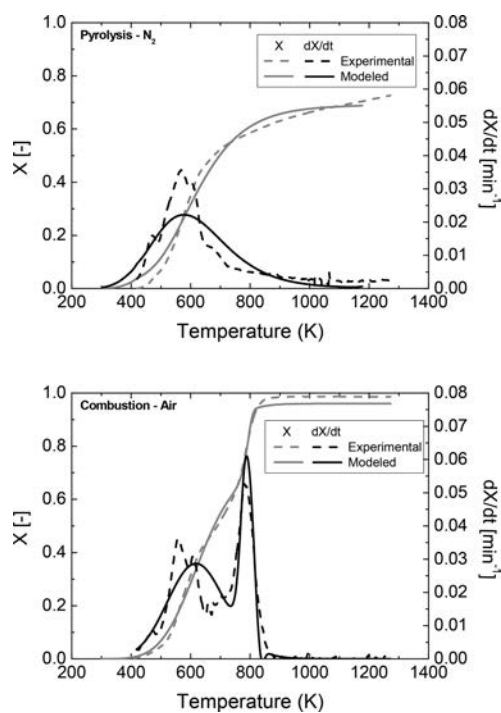
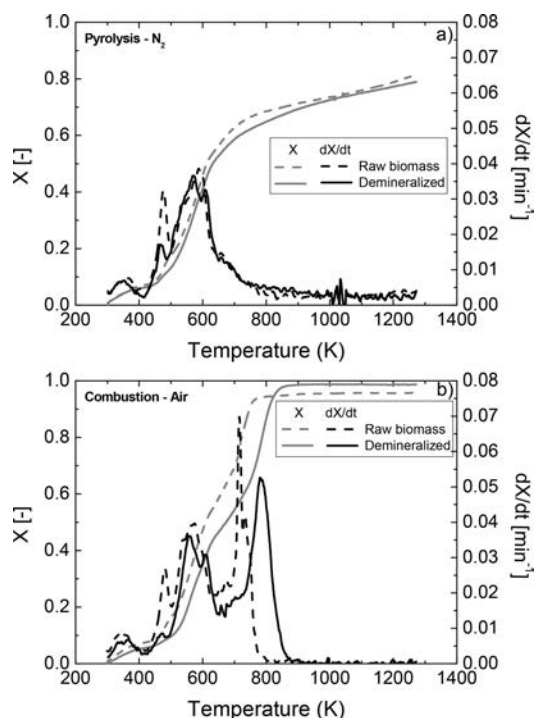


Figure 3. Typical pyrolysis and combustion profiles of the demineralized grape pomace. Experimental data, dashed lines; model data, continuous lines.

### 3. RESULTS AND DISCUSSION

**3.1. Influence of Potassium and Calcium on the Biomass Pyrolysis and Combustion Processes.** To analyze the reactivity of the biomass samples, the peak temperature ( $PT$ ), where the conversion rate is maximum,<sup>33</sup> is used. Considering a reference  $PT$ , it is found that the lower the peak temperature, the higher the reactivity of a fuel.

Figure 4 shows the conversion,  $X$ , and the conversion rate,  $dX/dt$ , versus the temperature of the raw grape pomace and the



**Figure 4.** (a) Pyrolysis in  $N_2$  and (b) combustion with air of raw and demineralized grape pomace up to 1275 K at 10 K/min in the TGA.

demineralized grape pomace during the pyrolysis and combustion processes.

The pyrolysis conversion profile of both biomass samples (Figure 4a) is characterized by an initial rapid decomposition, in the 425–650 K temperature interval, followed by a slower process up to a biomass conversion of about 0.8 at 1275 K. This process is related to the release of the volatile matter in biomass. The more rapid initial conversion profile is associated with the subsequent decomposition of hemicellulose and cellulose, and the latter conversion profile is attributed to the slow degradation of lignin.<sup>34</sup> The combustion conversion profile (Figure 4b) shows two rapid conversion stages separated by a gradual transition stage. As in the pyrolysis case, the first stage is related to the volatile matter release, while the second stage is related to a rapid char conversion enhanced by the oxygen in air. For both the raw and demineralized grape pomace, the main volatile matter release stage is finished at around 675 K. However, the char conversion stage is finished at 800 K for the raw biomass and 875 K for the demineralized biomass, pointing to a catalytic effect of metals during the char oxidation process. The demineralized biomass was fully consumed during its interaction with air (0.99 conversion), whereas the maximum conversion for the raw biomass is 0.96. This difference is attributed to the ash content of the raw grape

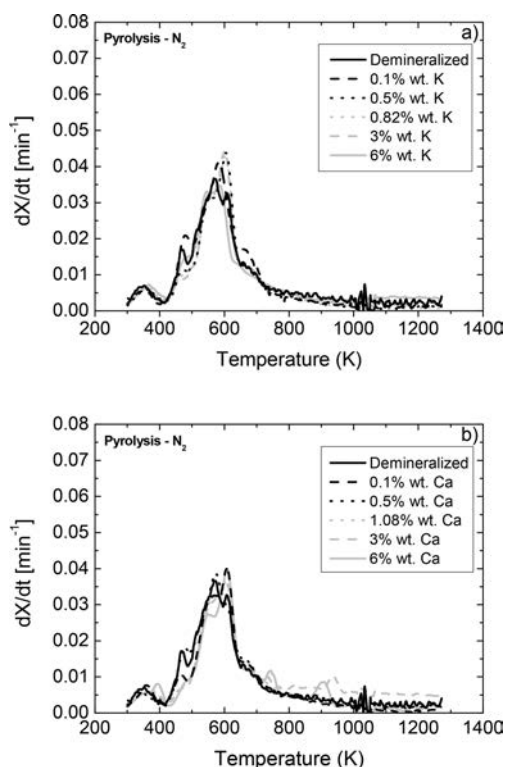
pomace (cf. Table 1) and supports the effectiveness of the demineralization process.

Figure 4 also shows the pyrolysis and combustion rates. After the first peak at 350 K that corresponds to the water release, for both the pyrolysis and combustion processes, the grape pomace devolatilization shows three distinct peaks. These peaks are generally associated with the release of the three main biomass components: hemicellulose (at 498–598 K), cellulose (at 598–648 K), and lignin (at 523–773 K).<sup>5</sup> The pyrolysis curve corresponding to the demineralized biomass shows the three peaks at the same temperature as in the case of the raw biomass, pointing to a marginal effect of the ash constituents of grape pomace on the characteristic temperatures of the volatile matter release. However, the magnitude of the peaks is slightly affected by the biomass demineralization treatment. The magnitude of the first peak, associated with hemicellulose, is the most affected. It substantially decreases when the biomass is demineralized. Previous studies<sup>35,36</sup> indicate that the demineralization processes, such as water or mild acid washing, can separate and sharpen the peaks of the rate curves. In the present work, the hemicellulose peak from the demineralized biomass is significantly decreased, up to almost disappearance, presumably as a result of its chemical degradation during the acid demineralization.<sup>37</sup>

The char oxidation stage exhibits one single peak stronger than the devolatilization general main peak. The mineral content of biomass influences the magnitude and temperature of the char oxidation peak; it is decreased and shifted to higher temperatures when the biomass was demineralized, reinforcing the catalytic effect of metals on char combustion.

To establish how the reactivity of the biomass is affected by the presence and concentration of K and Ca, the pyrolysis and combustion rates from the demineralized biomass are taken as a reference. Therefore, Figures 5 and 6 show the rate of mass loss for the demineralized grape pomace and all of the K- and Ca-doped biomass samples considered in this work during their pyrolysis and combustion, respectively. The conversion profiles used to draw data shown in Figures 5 and 6 are included as Figures 1S and 2S of the Supporting Information, respectively.

The general biomass pyrolysis profile (Figure 5) is neither influenced by the K nor Ca content. Independent of the K and Ca contents, the volatile matter release stage takes place in the 425–650 K temperature interval, with the main devolatilization peak within this range. In the case of the Ca-doped biomass samples, especially for the samples with 3 and 6 wt % Ca, the  $dX/dt$  profile shows two distinct peaks, at ~750 and ~925 K, respectively, that can be associated with the Ca transformations at a high temperature. The reactant used in the present work to dope the demineralized biomass with Ca is calcium oxalate monohydrate ( $CaC_2O_4 \cdot H_2O$ ). Its thermal decomposition involves dehydration, decomposition of calcium oxalate to calcium carbonate ( $CaCO_3$ ), and further decomposition of calcium carbonate to calcium oxide ( $CaO$ ).<sup>38</sup> Therefore, the characteristic peaks obtained would correspond to the decomposition of  $CaC_2O_4$  to  $CaCO_3$  and the subsequent formation of  $CaO$ . It is also interesting to note that the magnitude of the  $CaC_2O_4$  and  $CaCO_3$  decomposition peaks decreases as the amount of Ca used during the impregnation of the biomass decreases. As indicated in the Introduction, during a thermochemical process, Ca is released as small micrometer-sized  $CaO$  particles, which would support these observations.



**Figure 5.** Pyrolysis profiles of demineralized grape pomace and grape pomace doped with the different concentrations of (a) K and (b) Ca.

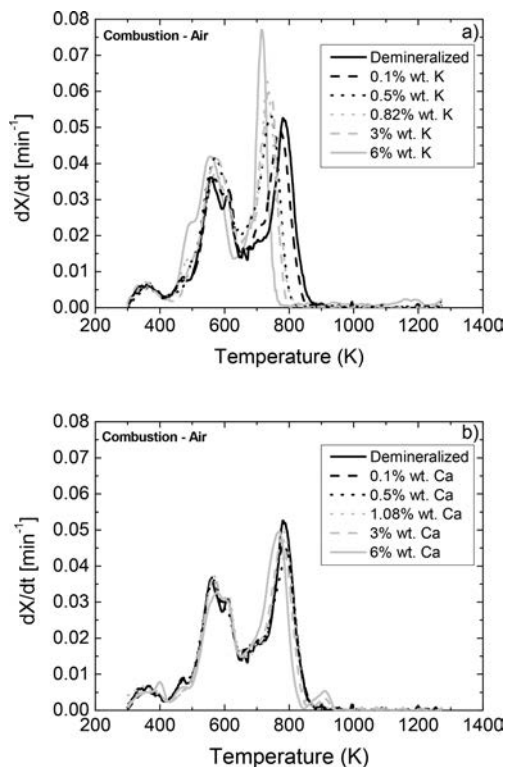


**Figure 6.** Combustion profiles of demineralized grape pomace and grape pomace doped with different concentrations of (a) K and (b) Ca.

In the case of biomass combustion (Figure 6), the main devolatilization peak is not significantly affected by the K and Ca contents of the biomass. However, K and Ca play a different role on the char oxidation process. In general, the char oxidation is promoted with an increasing K content, whereas Ca does not significantly influence this process. The char oxidation peak temperature is progressively shifted to lower temperatures, and its intensity increased as the K content of biomass is increased. For example, the peak temperature is shifted from 786 to 714 K with increasing the K content from demineralized biomass to 6 wt % K. These results are in line with the observations of Fuentes et al.<sup>27</sup> in relation to the catalytic effect of K on the char oxidation stage of biomass conversion and the lower activity of Ca. Moreover, these authors did not observed any effect of Ca on the volatile release stage. For the sample with 6 wt % K, it is interesting to note a small characteristic peak at ~1180 K, which can be related to the decomposition of potassium carbonate ( $K_2CO_3$ ) to potassium oxide ( $K_2O$ );<sup>12</sup> the thermal conversion of potassium oxalate monohydrate (reactant used to dope the biomass with K) involves dehydration and its decomposition to potassium carbonate ( $K_2CO_3$ ).<sup>38</sup> Table 2 summarized the characteristic temperatures of the volatile matter release and char oxidation regions.

Considering the results of the raw biomass sample and the biomass impregnated with similar amounts of K and Ca (i.e., 0.82 wt % K and 1.08 wt % Ca, respectively), it can be stated that neither K nor Ca is individually responsible for the catalytic effect of the mineral constituents of raw biomass, which points to a synergistic and/or cumulative effect of those minerals that actively catalyze the char oxidation stage of biomass combustion.

**3.2. Influence of Potassium and Calcium on the Biomass Ignition Temperature.** The minimum ignition temperature from TGA results can be determined by four different graphical methods: (i) the TG–DTG tangent method,<sup>39</sup> where the ignition temperature is defined by the intersection between the tangent to the TG curve at the main DTG peak and the horizontal line tangent to the TG curve after the water release peak (Figure 7a), (ii) the TG divergence method,<sup>40</sup> where the ignition temperature is defined by the separation of the pyrolysis and combustion TG curves (Figure 7b), (iii) the DTG decrease method,<sup>41</sup> where the ignition temperature is defined from the sudden decrease in the DTG curve after the water release stage (Figure 7c), and (iv) the DTG threshold method,<sup>42,43</sup> where the ignition temperature is determined by the 1%/min weight loss rate decrease after the water release stage (Figure 7d).

The characteristic ignition temperature depends strongly upon the specific graphical method used (see results shown in Figure 7), but results based on a consistent definition of the methodology and considering a reference case can be used to quantitatively compare the combustion behavior of biomass doped with different concentrations of K and Ca.

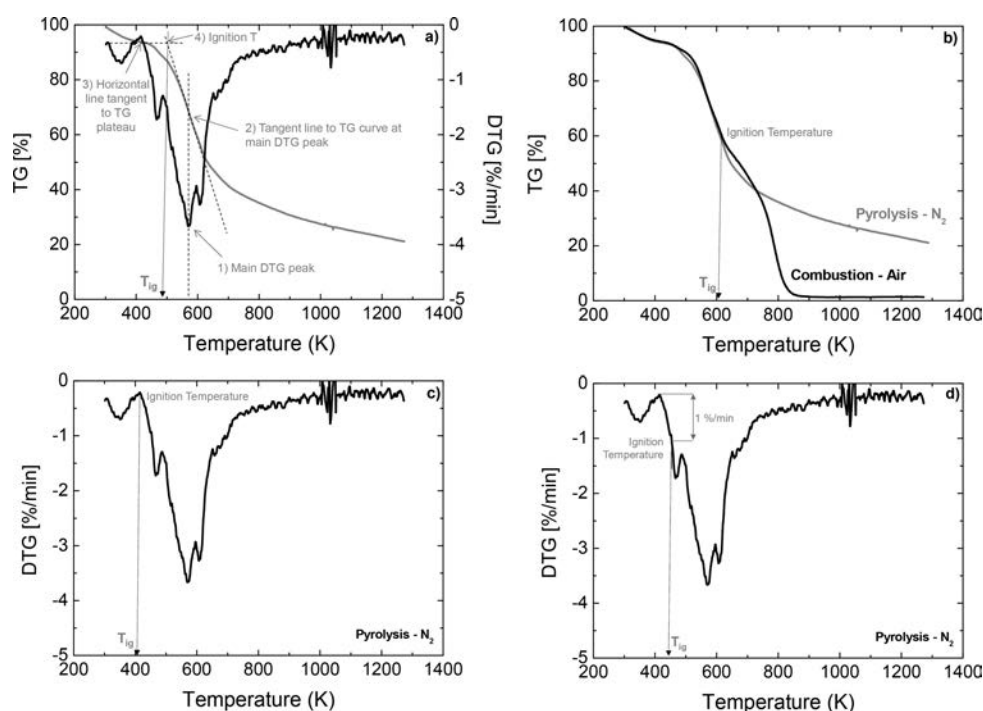
As discussed in section 3.1, the demineralization process affects the magnitude of the first peak after the water release stage, the hemicellulose peak. In the DTG threshold method, the ignition temperature is determined from the behavior of this first peak (see Figure 7d), and consequently, the results obtained with the biomass samples examined in the present work would not be reliable. Therefore, the DTG threshold method for the determination of the ignition temperature is not considered in this study.

For the K-doped biomass samples, the pyrolysis  $dX/dt$  profile does not show any additional peak associated with the presence of K or its concentration.

**Table 2. Characteristic Temperatures (K) of the Devolatilization Region of Pyrolysis and the Volatile Matter Release and Char Oxidation Regions of Combustion of the Raw and Demineralized Grape Pomace and Doped with the Different Concentrations of K and Ca<sup>a</sup>**

biomass sample	combustion								
	pyrolysis			devolatilization			char oxidation		
	$T_i$	$PT_{dev}$	$T_f$	$T_i$	$PT_{vol}$	$T_f$	$T_i$	$PT_{char}$	$T_f$
raw biomass	412	586	626	420	569	633	634	722	775
demineralized biomass	420	576	646	418	565	656	657	786	875
0.1 wt % K	400	583	637	420	572	652	653	772	853
0.5 wt % K	420	607	640	418	572	647	648	743	821
0.82 wt % K	420	607	637	420	572	641	642	736	825
3 wt % K	422	600	635	432	575	647	648	736	800
6 wt % K	420	586	626	418	558	631	632	714	775
0.1 wt % Ca	420	607	643	430	565	645	646	786	878
0.5 wt % Ca	415	572	641	424	569	652	653	793	878
1.08 wt % Ca	420	604	644	424	568	670	671	786	868
3 wt % Ca	424	607	640	428	569	649	650	779	860
6 wt % Ca	426	608	646	430	579	654	655	768	843

<sup>a</sup> $T_i$ , initial temperature of the stage;  $PT$ , peak temperature; and  $T_f$ , final temperature of the stage.



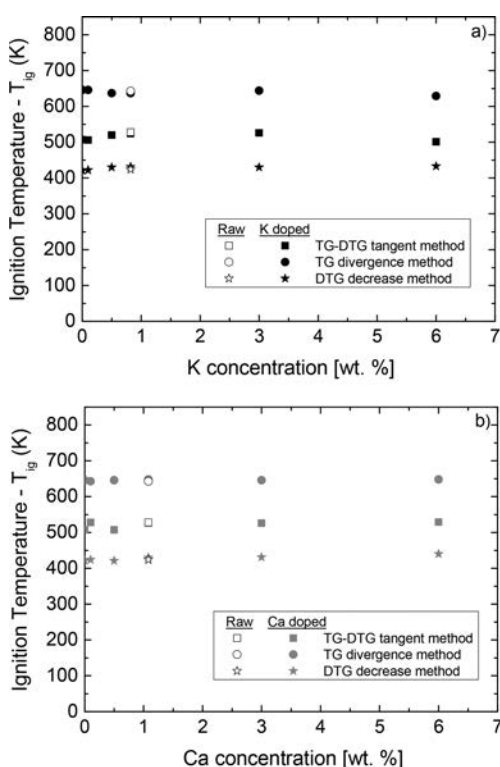
**Figure 7.** Graphical depiction of the (a) TG–DTG tangent method, (b) TG divergence method, (c) DTG decrease method, and (d) DTG threshold method used for the determination of the ignition temperature. Reference biomass is demineralized grape pomace.

Figure 8 shows the ignition temperature of the raw and demineralized grape pomace and doped with K and Ca. Independent of the method used for the determination of the  $T_{ig}$  data, the figure indicates that neither the demineralization process nor the presence of K and Ca (from low to high concentrations) significantly modifies the minimum ignition temperature of the biomass. For all biomass samples analyzed, the characteristic ignition temperatures ( $T_{ig}$ ) obtained with the DTG decrease method are in the order of 425 K, with the TG–DTG tangent method in the order of 515 K, and with the TG divergence method, the ignition temperatures increase further to values around 645 K.

**3.3. Influence of Potassium and Calcium on the Activation Energies.** Table 3 shows a summary of the kinetic

parameters (activation energy and pre-exponential factor) obtained for the devolatilization process during the biomass pyrolysis and the volatile matter release and char oxidation processes during the biomass combustion. The values reported in Table 3 are the averaged values from three runs for each biomass and condition. The variation of the coefficients reported for the activation energy values were in all cases lower than 10% for the pyrolysis process and lower than 2 and 2.2% for the devolatilization and char oxidation processes, respectively, during combustion.

For all of the samples analyzed, the pre-exponential factor values for the pyrolysis and devolatilization processes ( $A_V$ ) were in the order of  $10^{21}$  and the pre-exponential factor values for the char oxidation process during combustion ( $A_C$ ) were in the



**Figure 8.** Characteristic ignition temperatures of raw and demineralized grape pomace and doped with different concentrations of (a) K and (b) Ca.

order of  $10^{18}$ . The temperature power coefficient ( $\gamma$ ) laid within the  $-7.5$  to  $-6.5$  interval, independent of the process considered. In this work,  $\gamma$  is considered as an additional parameter for the fitting procedure; consequently, no further information is extracted from these values.

The pyrolysis process shows activation energies between 45 and 54 kJ/mol, and the devolatilization and char oxidation processes show activation energies between 58 and 68 kJ/mol and between 319 and 346 kJ/mol, respectively. The activation energy for the char oxidation is, in general, 5 times higher than that corresponding to the volatile matter release, which is in agreement with the different temperature windows for the occurrence of each of these stages (cf. Table 3). It is also

interesting to note that the activation energy of the volatile matter release process during the biomass combustion is quite similar to that corresponding to the biomass pyrolysis, which is in agreement with the similarity of the characteristic temperatures of both processes.

Figure 9 summarizes the individual activation energy of each biomass sample and process. In this figure, the data points with

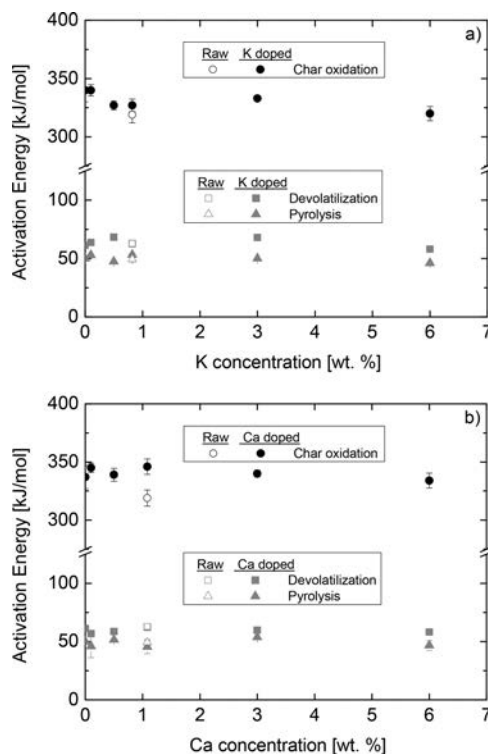


**Figure 9.** Activation energies of the pyrolysis and oxidation of raw and demineralized grape pomace and doped with different concentrations of (a) K and (b) Ca.

zero concentration correspond to the demineralized biomass sample, and the hollow symbols correspond to the raw biomass sample. The activation energy of the devolatilization process ( $E_V$ ) during both the pyrolysis and combustion of biomass is almost insensitive to the variation of the K and Ca

**Table 3.** Kinetic Parameters of Pyrolysis and Combustion of Raw Grape Pomace, Demineralized Grape Pomace, and Doped with Different Concentrations of K and Ca

biomass sample	combustion					
	pyrolysis		devolatilization		char oxidation	
	$E_V$ (kJ/mol)	$A_V$ ( $s^{-1}$ )	$E_V$ (kJ/mol)	$A_V$ ( $s^{-1}$ )	$E_C$ (kJ/mol)	$A_C$ ( $atm^{-1} s^{-1}$ )
raw biomass	49.4	$3.79 \times 10^{21}$	63.0	$2.18 \times 10^{21}$	319	$4.84 \times 10^{18}$
demineralized biomass	50.0	$7.91 \times 10^{21}$	61.5	$7.40 \times 10^{21}$	340	$1.92 \times 10^{18}$
0.1 wt % K	53.0	$2.10 \times 10^{21}$	63.5	$4.60 \times 10^{21}$	340	$4.56 \times 10^{18}$
0.5 wt % K	47.4	$3.30 \times 10^{21}$	68.0	$5.38 \times 10^{21}$	327	$5.39 \times 10^{18}$
0.82 wt % K	53.2	$3.09 \times 10^{21}$	63.0	$7.66 \times 10^{21}$	327	$5.54 \times 10^{18}$
3 wt % K	50.2	$8.84 \times 10^{21}$	67.8	$3.93 \times 10^{21}$	333	$7.85 \times 10^{18}$
6 wt % K	46.2	$5.50 \times 10^{21}$	58.1	$6.37 \times 10^{21}$	320	$4.33 \times 10^{18}$
0.1 wt % Ca	46.0	$4.55 \times 10^{21}$	56.8	$8.18 \times 10^{21}$	345	$4.66 \times 10^{18}$
0.5 wt % Ca	51.7	$7.71 \times 10^{21}$	58.7	$3.42 \times 10^{21}$	339	$1.45 \times 10^{18}$
1.08 wt % Ca	45.5	$3.77 \times 10^{21}$	62.3	$7.21 \times 10^{21}$	346	$7.12 \times 10^{18}$
3 wt % Ca	53.8	$5.84 \times 10^{21}$	59.8	$4.63 \times 10^{21}$	340	$2.31 \times 10^{18}$
6 wt % Ca	46.7	$3.83 \times 10^{21}$	58.2	$5.33 \times 10^{21}$	334	$3.82 \times 10^{18}$

concentrations of biomass, but the activation energy of the char oxidation process ( $E_C$ ) during the combustion of biomass is somewhat sensitive to the mineral content of biomass. In this way, the activation energy of the char oxidation stage from the combustion of the demineralized biomass sample is 6.6% higher than the  $E_C$  value of the raw sample of grape pomace.

In the case of K (Figure 9a), the activation energy of the char oxidation process ( $E_C$ ) decreases with the increase of the K concentration until the 0.5 wt % K sample and continues slightly decreasing further up to 6 wt % K, where the  $E_C$  value is similar to that corresponding to the raw grape pomace sample. As for the devolatilization process, Ca (Figure 9b) has a marginal effect on the activation energy of the char oxidation process. The  $E_C$  value for the biomass samples with different Ca concentrations is very close to the  $E_C$  value of the demineralized biomass.

#### 4. CONCLUSION

The individual role of the presence and concentration of K and Ca in the combustion characteristics of grape pomace has been analyzed. The grape pomace was demineralized and, subsequently, doped with K and Ca to obtain doped samples that covered a wide and realistic concentration range of both minerals in different biomass fuels. Specifically, this work includes the analysis of the pyrolysis and oxidation processes in a TGA of raw and demineralized grape pomace and demineralized biomass doped with 0.1, 0.5, 0.82, 3, and 6 wt % K and 0.1, 0.5, 1.08, 3, and 6 wt % Ca.

In general, neither the ignition temperature nor the devolatilization process of biomass is significantly affected by the presence of K and Ca contents lower than 6 wt %. The char oxidation was promoted by the presence of K, with a more noticeable effect as the K concentration in the biomass was increased. In this case, the char oxidation profile of the biomass doped with 6 wt % K was shifted 72 K to lower temperatures compared to the demineralized biomass.

The activation energies for the volatile matter release during the pyrolysis and oxidation of biomass were in the intervals of 45–54 and 58–69 kJ/mol, respectively, while for char oxidation, it was in the interval of 318–346 kJ/mol. The impact of the mineral content of biomass is more significant on the char oxidation process of biomass combustion than on the pyrolysis and devolatilization processes. Neither high concentrations of Ca and K (up to 6 wt % of each individual mineral) nor the minerals present in the raw grape pomace influence the activation energy of the pyrolysis and devolatilization process of biomass combustion. The minerals present in the raw grape pomace and K individually show a catalytic effect on the activation energy of the char oxidation process. This effect is promoted by increased K concentrations. On the contrary, under the conditions of the present work, Ca behaves as an inert.

#### ASSOCIATED CONTENT

##### Supporting Information

The Supporting Information is available free of charge on the ACS Publications website at DOI: 10.1021/acs.energyfuels.7b02161.

Pyrolysis in  $N_2$  of demineralized grape pomace and grape pomace doped with different concentrations of (a) K and (b) Ca (Figure 1S) and combustion with air of demineralized grape pomace and grape pomace doped

with different concentrations of (a) K and (b) Ca (Figure 2S) (PDF)

#### AUTHOR INFORMATION

##### Corresponding Author

\*E-mail: [mabian@unizar.es](mailto:mabian@unizar.es).

##### ORCID

M. Abián: 0000-0001-7559-9669

M. U. Alzueta: 0000-0003-4679-5761

##### Notes

The authors declare no competing financial interest.

#### ACKNOWLEDGMENTS

The work was funded by MINECO and FEDER (Project CTQ2015-65226) and Fundação para a Ciência e a Tecnologia (FCT), through IDMEC, under LAETA Pest-OE/EME/LA0022 and PTDC/EMS-ENE/5710/2014. M. Abián acknowledges MINECO and Instituto de Carboquímica (ICB-CSIC) for the postdoctoral grant awarded (FPDI-2013-16172) and Fundaciones Ibercaja y CAI (Program Ibercaja-CAI for research stays) and COST Action CM1404 (EU) for financial support (reference ECOST-STSM-CM1404-010716-079613).

#### REFERENCES

- Niu, Y.; Tan, H.; Hui, S. *Prog. Energy Combust. Sci.* **2016**, *52*, 1–61.
- Glarborg, P. *Proc. Combust. Inst.* **2007**, *31*, 77–98.
- Di Blasi, C. *Prog. Energy Combust. Sci.* **2008**, *34*, 47–90.
- Tortosa-Masiá, A. A.; Buhre, B. J. P.; Gupta, R. P.; Wall, T. F. *Fuel Process. Technol.* **2007**, *88*, 1071–1081.
- Nunes, L. J. R.; Matias, J. C. O.; Catalão, J. P. S. *Renewable Sustainable Energy Rev.* **2016**, *53*, 235–242.
- Vassilev, S. V.; Baxter, D.; Andersen, L. K.; Vassileva, C. G. *Fuel* **2010**, *89*, 913–933.
- Niu, Y.; Zhu, Y.; Tan, H.; Hui, S.; Jing, Z.; Xu, W. *Fuel Process. Technol.* **2014**, *128*, 499–508.
- Lindstrom, E.; Sandstrom, M.; Bostrom, D.; Ohman, M. *Energy Fuels* **2007**, *21*, 710–717.
- Lindstrom, E.; Ohman, M.; Backman, R.; Bostrom, D. *Energy Fuels* **2008**, *22*, 2216–2220.
- Jones, J. M.; Darvell, L. I.; Bridgeman, T. G.; Pourkashanian, M.; Williams, A. *Proc. Combust. Inst.* **2007**, *31*, 1955–1963.
- Blomberg, T. *Mater. Corros.* **2011**, *62*, 635–641.
- Lehman, R. L.; Gentry, J. S.; Glumac, N. G. *Thermochim. Acta* **1998**, *316*, 1–9.
- Veksha, A.; Zaman, W.; Layzell, D. B.; Hill, J. M. *Bioresour. Technol.* **2014**, *171*, 88–94.
- Raveendran, K.; Ganesh, A.; Khilar, K. C. *Fuel* **1995**, *74*, 1812–1822.
- Nowakowski, D. J.; Jones, J. M. *J. Anal. Appl. Pyrolysis* **2008**, *83*, 12–25.
- Zhao, D.; Chen, K.; Yang, F.; Feng, G.; Sun, Y.; Dai, Y. *Cellulose* **2013**, *20*, 3205–3217.
- Zolin, A.; Jensen, A.; Jensen, P. A.; Frandsen, F.; Dam-Johansen, K. *Energy Fuels* **2001**, *15*, 1110–1122.
- Fahmi, R.; Bridgwater, A. V.; Darvell, L. I.; Jones, J. M.; Yates, N.; Thain, S.; Donnison, I. S. *Fuel* **2007**, *86*, 1560–1569.
- Nowakowski, D. J.; Jones, J. M.; Brydson, R. M. D.; Ross, A. B. *Fuel* **2007**, *86*, 2389–2402.
- Dall’Ora, M.; Jensen, P. A.; Jensen, A. D. *Energy Fuels* **2008**, *22*, 2955–2962.
- Boström, D.; Skoglund, N.; Grimm, A.; Boman, C.; Öhman, M.; Boström, M.; Backman, R. *Energy Fuels* **2012**, *26*, 85–93.
- Pan, W.-P.; Richards, G. N. *J. Anal. Appl. Pyrolysis* **1989**, *16*, 117–126.

- 559 (23) Aho, A.; DeMartini, N.; Pranovich, A.; Krogell, J.; Kumar, N.;  
560 Eränen, K.; Holmbom, B.; Salmi, T.; Hupa, M.; Murzin, D. Yu.  
561 *Bioresour. Technol.* **2013**, *128*, 22–29.
- 562 (24) Leventis, Y. A.; Nam, S. W.; Lowenberg, M.; Flagan, R. C.;  
563 Gavalas, G. R. *Energy Fuels* **1989**, *3*, 28–37.
- 564 (25) Gopalakrishnan, R.; Fullwood, M. J.; Bartholomew, C. H. *Energy*  
565 *Fuels* **1994**, *8*, 984–989.
- 566 (26) Gopalakrishnan, R.; Bartholomew, C. H. *Energy Fuels* **1996**, *10*,  
567 689–695.
- 568 (27) Fuentes, M. E.; Nowakowski, F. J.; Kubacki, M. L.; Cove, J. M.;  
569 Bridgeman, T. G.; Jones, J. M. *J. Energy Inst.* **2008**, *81*, 234–241.
- 570 (28) Perander, M.; DeMartini, N.; Brink, A.; Kramb, J.; Karlström,  
571 O.; Hemming, J.; Moilanen, A.; Konttinen, J.; Hupa, M. *Fuel* **2015**,  
572 *150*, 464–472.
- 573 (29) White, J. E.; Catallo, W. J.; Legendre, B. L. *J. Anal. Appl. Pyrolysis*  
574 **2011**, *91*, 1–33.
- 575 (30) Ferreiro, A. I.; Rabaçal, M.; Costa, M. *Energy Convers. Manage.*  
576 **2016**, *125*, 290–300.
- 577 (31) Di Blasi, C. *Prog. Energy Combust. Sci.* **2009**, *35*, 121–140.
- 578 (32) Hurt, R. H.; Calo, J. M. *Combust. Flame* **2001**, *125*, 1138–1149.
- 579 (33) Cumming, J. W. *Fuel* **1984**, *63*, 1436–1440.
- 580 (34) Yang, H.; Yan, R.; Chen, H.; Lee, D. H.; Zheng, C. *Fuel* **2007**,  
581 *86*, 1781–1788.
- 582 (35) Di Blasi, C.; Branca, C.; D’Errico, G. *Thermochim. Acta* **2000**,  
583 *364*, 133–142.
- 584 (36) Stenseng, M.; Jensen, A.; Dam-Johansen, K. *J. Anal. Appl.*  
585 *Pyrolysis* **2001**, *58–59*, 765–780.
- 586 (37) Eom, I.-Y.; Kim, J.-Y.; Kim, T.-S.; Lee, S.-M.; Choi, D.; Choi, I.-  
587 G.; Choi, J.-W. *Bioresour. Technol.* **2012**, *104*, 687–694.
- 588 (38) Dollimore, D. *Thermochim. Acta* **1987**, *117*, 331–363.
- 589 (39) Li, Q.; Zhao, C.; Chen, X.; Wu, W.; Li, Y. *J. Anal. Appl. Pyrolysis*  
590 **2009**, *85*, 521–528.
- 591 (40) Ma, B.-G.; Li, X.-G.; Xu, L.; Wang, K.; Wang, X.-G. *Thermochim.*  
592 *Acta* **2006**, *445*, 19–22.
- 593 (41) Jones, J. M.; Lea-Langton, A. R.; Ma, L.; Pourkashanian, M.;  
594 Williams, A. *Pollutants Generated by the Combustion of Solid Biomass*  
595 *Fuels*; Springer: London, U.K., 2014; DOI: [10.1007/978-1-4471-6437-](https://doi.org/10.1007/978-1-4471-6437-596)  
596 [1](https://doi.org/10.1007/978-1-4471-6437-596).
- 597 (42) Faúndez, J.; Arenillas, A.; Rubiera, F.; García, X.; Gordon, A. L.;  
598 Pis, J. J. *Fuel* **2005**, *84*, 2172–2177.
- 599 (43) Moon, C.; Sung, Y.; Ahn, S.; Kim, T.; Choi, G.; Kim, D. *Appl.*  
600 *Therm. Eng.* **2013**, *54*, 111–119.